Cellular Physiology and Biochemistry

Cell Physiol Biochem 2018;47:1167-1180
DOI: 10.1159/000490213
Published online: June 18, 2018
Accepted: April 10, 2018

Original Paper

Rapid Electrical Stimulation Increased Cardiac Apoptosis Through Disturbance of Calcium Homeostasis and Mitochondrial Dysfunction in Human Induced Pluripotent Stem Cell-Derived Cardiomyocytes

Le Geng[a] Zidun Wang[a] Chang Cui[a] Yue Zhu[a] Jiaojiao Shi[a] Jiaxian Wang[a] Minglong Chen[a]

[a]The First Affiliated Hospital of Nanjing Medical University, Nanjing, China

Key Words
Rapid electrical stimulation • HiPSC-CMs • Calcium homeostasis • Mitochondria • Apoptosis • CaMKII

Abstract
Background/Aims: Heart failure induced by tachycardia, the most common arrhythmia, is frequently observed in clinical practice. This study was designed to investigate the underlying mechanisms. ***Methods:*** Rapid electrical stimulation (RES) at a frequency of 3 Hz was applied on human induced pluripotent stem cell-derived cardiomyocytes (hiPSC-CMs) for 7 days, with 8 h/day and 24 h/day set to represent short-term and long-term tachycardia, respectively. Age-matched hiPSC-CMs without electrical stimulation or with slow electrical stimulation (1 Hz) were set as no electrical stimulation (NES) control or low-frequency electrical stimulation (LES) control. Following stimulation, JC-1 staining flow cytometry analysis was performed to examine mitochondrial conditions. Apoptosis in hiPSC-CMs was evaluated using Hoechst staining and Annexin V/propidium iodide (AV/PI) staining flow cytometry analysis. Calcium transients and L-type calcium currents were recorded to evaluate calcium homeostasis. Western blotting and qPCR were performed to evaluate the protein and mRNA expression levels of apoptosis-related genes and calcium homeostasis-regulated genes. ***Results:*** Compared to the controls, hiPSC-CMs following RES presented mitochondrial dysfunction and an increased apoptotic percentage. Amplitudes of calcium transients and L-type calcium currents were significantly decreased in hiPSC-CMs with RES. Molecular analysis demonstrated upregulated expression of Caspase3 and increased Bax/Bcl-2 ratio. Genes related to calcium re-sequence were downregulated, while phosphorylated Ca^{2+}/calmodulin-dependent protein kinase II (CaMKII) was significantly upregulated following RES. There was no significant difference between the NES control and LES control groups in these aspects. Inhibition of CaMKII with 1 μM KN93 partly reversed these adverse effects of RES. ***Conclusion:*** RES on hiPSC-CMs disturbed calcium homeostasis, which led to mitochondrial stress, promoted cell apoptosis and caused

L. Geng, Z. Wang and C Cui contributed equally to this work.

Minglong Chen, MD

Division of Cardiology, The First Affiliated Hospital of Nanjing Medical University
Nanjing 210029 (China)
Tel. 0086-25-68136965, Fax 0086-25-6813-6479, E-Mail chenminglong@njmu.edu.cn

electrophysiological remodeling in a time-dependent manner. CaMKII played a central role in the damages induced by RES, pharmacological inhibition of CaMKII activity partly reversed the adverse effects of RES on both structural and electrophysiological properties of cells.

Introduction

Tachycardia is the most common arrhythmia, which can cause many negative outcomes, including heart failure or even sudden cardiac death (SCD) in some patients [1]. Although various treatment procedures have been undertaken to terminate tachycardia, including drug prescription and ablations [2], several studies have claimed that some patients still suffer higher risks of congestive heart failure, recurrence of tachycardia, and SCD even after the termination of tachycardia, indicating some remained damages induced by tachycardia [3, 4].

Despite the fact that several animal models have been created to investigate the mechanisms by which tachycardia cause heart dysfunction [5-7], little is known about the changes occurring at the cellular level and the underlying mechanisms. To handle this issue, several researchers have applied rapid electrical stimulation (RES) on cardiomyocytes. Due to the difficulties in obtaining human adult cardiomyocytes, cardiomyocytes used in these trials were primarily isolated from rats [8] and mice [9, 10]. However, considering the significant species differences and the inherent defect of isolated cells wherein they cannot be cultivated long-term, it remains debatable whether these observations are applicable to human beings.

Human induced pluripotent stem cell-derived cardiomyocytes (hiPSC-CMs) have been obtained and applied in many studies [11, 12], and have been demonstrated the similar properties to human myocardia in several aspects, including ion channel gene expressions [13, 14], sarcoplasmic reticulum (SR) calcium handling [15, 16], etc. Based on the abovementioned hurdles and the advantages of regenerative cardiomyocytes, we sought to investigate the changes brought about by tachycardia and the underlining mechanisms by applying RES on hiPSC-CMs.

Herein, compared to the no electrical stimulation (NES) control group and low-frequency electrical stimulation (LES) control group, RES disturbed calcium homeostasis and activated the mitochondrial apoptotic pathway(MAP), which may lead to cardiomyocyte loss and systolic dysfunction. Phosphorylated Ca^{2+}/calmodulin-dependent protein kinase II (p-CaMKII) was upregulated following RES, and inhibition of CaMKII partly reversed the adverse effects of RES, including disturbed calcium transients, decreased L-type calcium currents and cardiomyocyte apoptosis. Therefore, CaMKII could potentially be chosen as a supplemental therapeutic target for tachycardia patients.

Materials and Methods

Stem cells culture and differentiation

Human iPSC line NC5 cells (Help Stem Cell Innovations, NC2001) were seeded onto Matrigel (Corning, Corning, NY, USA, 354277) coated 6-well plates and cultured in the mTeSR™ medium (StemCell Technologies, Vancouver, Canada, 05850) to 90% cell confluency. Next, NC5 hiPSCs were differentiated to cardiomyocytes as previously described by our group [17]. Eight weeks following the differentiation, cells were digested with 0.25% trypsin-EDTA (Life Technologies) and resuspended into single-cell suspension and reseeded on gelatin-coated plates for further study.

Generation of the electrical stimulation model

hiPSC-CMs were reseeded onto 6-well plates at appropriate concentrations. Electrical stimulation was conducted using a CDish100™ culture dish and C-Pace100™ culture pacer (IonOptix Corporation, Netherlands). For RES, 3 V, 0.5 ms and 3 Hz of electrical pulses were selected. Two subgroups—8 h/day

(S-8h) and 24 h/day (S-24h)—were set to represent short-term and long-term tachycardia. To examine whether electrical stimulation itself can bring about any changes to cardiomyocytes, stimulation at 1 Hz frequency for 24 h/day was applied to a group of cells as the low electrical stimulation (LES) control group. Age-matched cardiomyocytes without electrical stimulation were used as no electrical stimulation (NES) controls. After 7 days of stimulation, cardiomyocytes were harvested for functional assessments.

Measurement of mitochondrial membrane potential

Mitochondrial membrane potential (MMP) was measured with the fluorescent indicator JC-1 (Beyotime Institute of Biotechnology, China, C2006). In normal cells, JC-1 forms aggregates which fluoresce with an emission peak at 588 nm. Decreased membrane potential favors the monomers of JC-1, which has an emission peak at 530 nm. Cardiomyocytes were harvested using 0.25% trypsin. Approximately 100, 000 cells were suspended in 0.5 mL medium in each tube for JC-1 staining. Staining working solution was prepared following the manufacturer's instructions. Five hundred microliters of the working solution were added into each tube and cardiomyocytes were incubated for 20 min at 37°C in the dark. Following incubation, cells were washed with JC-1 staining buffer twice and resuspended for flow cytometry analysis. The wavelengths of excitation and emission were 514 nm/529 nm for detection of the monomers form of JC-1, and 585 nm/590 nm for detection of the aggregates through FL-1 and FL-2 channels.

Hoechst staining

Hoechst staining (Beyotime Institute of Biotechnology, China, C0003) was used to evaluate morphological features of cardiomyocytes. Cells were washed with cold DPBS and fixed in prepared 4% PFA for 30 min. After fixation, cells were washed with cold DPBS twice and incubated with 5 μg/ml Hoechst at 37°C for 15 min in the dark. Following incubation, cells were washed again and apoptotic cells were identified using a fluorescence microscope (Axio Vert.A1, Zeiss). Normal cells presented homogeneous blue chromatin, while apoptotic cells were bright blue condensed or fragmented.

Flow cytometry for apoptosis analysis

Annexin V/propidium iodide (AV/PI) staining was used, according to manufacturer's instructions, to evaluate cell apoptosis. Briefly, approximately 1×10^6 cells were harvested with 0.25% trypsin without EDTA and resuspended in 300 μL binding buffer. Next, cells were incubated with AV/PI (Vazyme Biotech Company, China, A211-02) for 20 min in the dark and analyzed with a flow cytometer (BD FACS Calibur) within 1 hour. Data from 8, 000 cells/sample were collected, and quadrants were set according to viable, unstained populations in blank samples.

Measurement of calcium transients

Following the manufacture's instruction, Fluo-3 AM (Life technology, F1242) was used to measure calcium transients. In brief, 5 mM Fluo-3 AM in DMSO stock and equal volume of 20% (w/v) Pluoronic F-127 were diluted to 5 μM using culture medium to obtain the working solution. Cells were washed with DPBS twice before being incubated with the working solution for 90 min at 37°C. After incubation, cells were washed to remove any remaining dye and then incubated with normal culture medium for another 30 min. Next, cells were washed again and medium was changed to Tyrode's solution. Fluo-3 AM in the cardiomyocytes was excited at a light wavelength of 488 nm and the emission was recorded at 520 nm using a E3CMOS camera (Touptek, China). The Ca^{2+} transients are expressed as $\Delta F/F_0$, where ΔF is the change in fluorescence intensity relative to the minimal fluorescence (F_0) measured at each Ca^{2+} transient.

Patch-clamp recordings

Whole-cell patch clamp was used to record the L-type calcium currents ($I_{Ca,L}$) of cardiomyocytes on the Axopatch 200B amplifier (Axon Instruments, CA, USA) at 37°C, as previously described [17]. Patch pipettes were prepared with a micropipette puller (P-1000, Sutter Instrument, Novato, CA, USA) and had a typical resistance of 3-6 MΩ. $I_{Ca,L}$ was examined using the following intracellular solution: 130 mM CsCl, 20 mM TEA-Cl, 1.8 mM $MgCl_2$, 5 mM Na_2ATP, 5 mM EGTA, 10 mM glucose, and 10 mM HEPES (pH 7.3 with CsOH). The external bath solution composition was as follows: 120 mM choline chloride, 20 mM CsCl, 1 mM $MgCl_2$, 1.8 mM $CaCl_2$, 10 mM glucose, and 10 mM HEPES (pH 7.3 with CsOH). The program for recording $I_{Ca,L}$ was from a holding potential of −40 mV to measure potentials from −40 to +60 mV, every 10 mV for 500 ms. Cell

capacitance was used to normalize $I_{Ca,L}$ and current density were expressed as pA/pF. Data were analyzed using Clampfit 10.6 (Axon Instruments).

Quantitative RT-PCR

Total RNA was extracted with the TRIzol Reagent (Invitrogen) following the manufacturer's instructions. Amounting to 500 ng RNA was used for the synthesis of cDNA using a SuperScript Reverse Transcriptase (Bio-Rad, Hercules, CA, USA, 170-8891). qRT-PCR was performed using the AB 7900HT Real-Time PCR System (ABI, USA) with SYBR Green (Bio-Rad, 170-8882AP) in a total reaction series of 10 μL mixture. mRNA levels were based on the critical threshold (Ct) value and were normalized to Glyceraldehyde-3-phosphate dehydrogenase (GAPDH). The primers used in this work (for all online suppl. material, see www.karger.com/doi/10.1159/000490213) are listed in Table S1.

Western Blotting

Western blotting was conducted as previously described by our group [17]. The primary antibodies used in the present study were as follows: GAPDH (1:1000, Cell Signaling, 2118S), Bcl-2 (1:1000, Cell Signaling, 3498), Caspase-3 (1:1000, Cell Signaling, 9662), Bax (1:1000, Cell Signaling, 2772), Serca2a (1:1000, Abcam, ab2861), Phospholamban (1:1000, Abcam, ab15000), p-CaMKII (1:1000, Cell Signaling, 12716T), and Calsequestrin-2 (1:1000, Abcam, ab108289). Secondary antibodies employed in this work included anti-rabbit IgG antibody (1:5000, Cell Signaling, 7074P2) or anti-mouse IgG antibody (1:5000, Cell Signaling, 7076).

Immunofluorescent staining

Immunofluorescent staining was performed as previously described by our group [17]. Approximately 30, 000 hiPSC-CMs were reseeded onto gelatin-coated 24mm coverslips and electrical stimulation began at different parameters 3 days after the seeding. After the stimulation, cardiomyocytes were fixed and permeabilized before being blocked with 5% BSA. After the incubation with primary antibody cTnT (1:200, Abcam, ab8295) at 4°C overnight, cells were washed and incubated with fluorescent-conjugated secondary antibody (1:500, Abcam, ab150077) at room temperature in the dark for 1 hour. Nuclei were stained with DAPI (Life Technologies, P36931) for 10 min at room temperature before observed and captured by a Zeiss fluorescence microscope (Axio Imager A2, Zeiss).

Statistical analysis

All results were expressed as the Means ± standard deviation (SD). SPSS Statistics 19.0 (IBM Corp., Armonk, NY, USA) was used for Statistical analysis. One-way analysis of variance (ANOVA) was performed for testing significant differences among experimental groups. A p value less than 0.05 was considered statistically significant.

Results

RES decreased mitochondrial membrane potential (MMP)

It was accepted that tachycardia could alter the mitochondrial metabolism [18, 19]. Recently, Karin A.L. Mueller et al. [20] reported a disturbed mitochondrion distribution in cardiomyocytes from tachycardia patient biopsies. Therefore, we first examined mitochondrial function at the cellular level. Mitochondrial membrane potential (MMP) is an indicator of mitochondrial function, and loss of MMP often suggests mitochondrial dysfunction. Flow cytometry analysis of JC-1 staining demonstrated a significantly decreased fluorescence intensity of aggregates and an increased fluorescence intensity of monomers (Fig. 1A). The ratio of monomers and aggregates significantly increased from 0.45±0.06 in the NES control group to 1.21±0.24 (p<0.01) in S-8 h group and 2.17±0.32 (p<0.001) in S-24 h group, indicating a dramatic loss in MMP and resultant mitochondrial dysfunction in the rapid stimulation groups (Fig. 1B). There was no significant increase in the LES control group (0.49±0.07, p=0.53) compared to the NES control group.

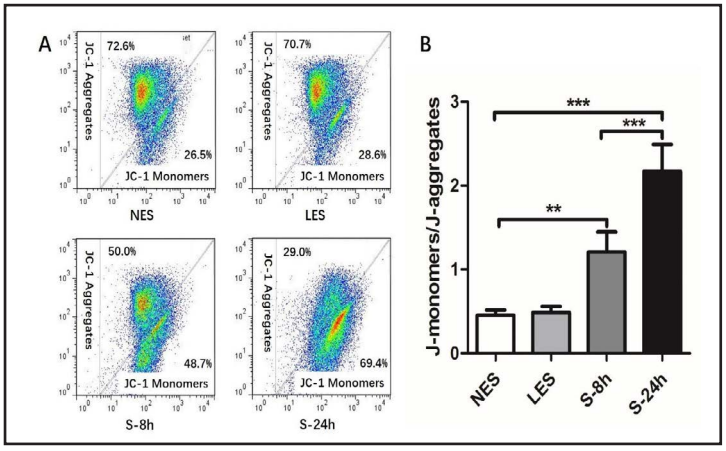

Fig. 1. RES decreased mitochondrial membrane potential (MMP). A: Representative flow cytometry analysis of JC-1 staining. Electrical stimulation parameters of each experimental group are listed as follows: NES control: no electrical stimulation. LES: low-frequency electrical stimulation. 3 V, 0.5 ms, 1 Hz, 24 h/day, 7 days. S-8 h: 3 V, 0.5 ms, 3 Hz, 8 h/day, 7 days. S-24 h: 3 V, 0.5 ms, 3 Hz, 24 h/day, 7 days. Horizontal axis and Vertical axis represent fluorescence intensities of JC-1 monomers and JC-1 aggregates, respectively. Increased intensity of monomers indicates decreased MMP. B: Ratio of JC-1 monomers and aggregates is presented as the Mean ± SD of 4 independent experiments. Ratios were significantly increased in RES groups in a time-dependent manner. **p<0.01, ***p<0.001 tested by one-way ANOVA.

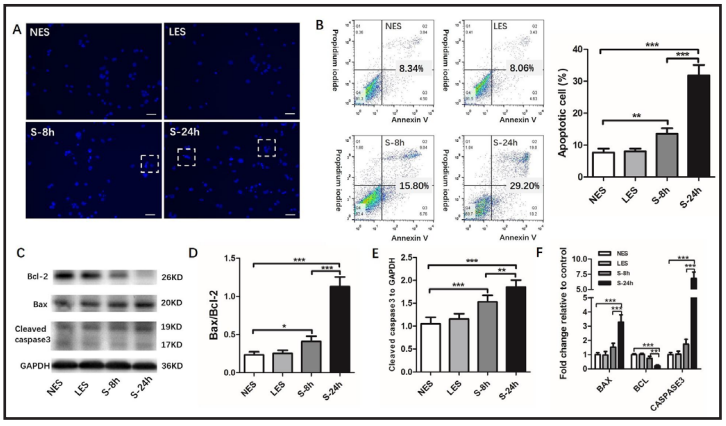

Fig. 2. RES promoted cardiomyocyte apoptosis. A: Cardiomyocyte apoptosis observed using Hoechst staining. Representative morphological changes in apoptosis, such as shrunken cells with fragmented or condensed nuclei, and are indicated by dotted boxes (Scar bar 50 μm). B: Representative flow cytometry analysis of AV/PI staining. Percentage of upper-right and lower-right quadrants of each image were summed as total apoptotic percentage and presented in the histogram as the Mean ± SD of 4 independent experiments. There were significant higher percentages of apoptotic cells following RES. C: Representative western blotting image of apoptosis-related proteins. Following RES, protein levels of cleaved caspase3 and pro-apoptotic Bax were significantly upregulated and those of anti-apoptotic Bcl-2 were correspondingly downregulated in a time-dependent manner. GAPDH was used as an internal control. D: Ratio of protein density of pro-apoptotic Bax to anti-apoptotic Bcl-2. Ratios were significantly increased in RES groups(n=4). E: Protein density of cleaved Capase3 relative to GAPDH. Expression of cleaved Capase3 was significantly upregulated following RES in a time-dependent manner(n=4). F: qPCR analysis of apoptosis-related genes(n=3). *p<0.05, **p<0.01, ***p<0.001 tested by one-way ANOVA.

RES promoted cardiomyocyte apoptosis

Biopsies from tachycardia patients [21, 22] and animal models [23] showed decreased cardiomyocytes and increased fibrotic tissues, but little is known about the underlying mechanisms. Considering that our previous study demonstrated increased apoptosis in HL-1 cells after rapid pacing [10], we next examined the morphological features of cell nuclei using Hoechst staining. Cardiomyocytes in S-8 h group and S-24 h group exhibited the typical morphological characteristics of apoptosis including condensed or fragmented nuclei after 7 days of RES compared to the NES control group (Fig. 2A). In order to further quantify the apoptotic rates, flow cytometry analysis of apoptosis was performed using the AV/PI staining

(Fig. 2B). Similar to the results of Hoechst staining, RES significantly increased the apoptotic cell percentage in a time-dependent manner (7.69±1.22%, 13.56±1.74%, 31.85±3.27% for NES control, S-8 h and S-24 h groups, respectively, $p<0.001$). In contrast, there was no significant difference between cardiomyocytes in the NES control group and the LES control group (8.06±0.86%, $p=0.64$).

Since several studies have emphasized the relationship between mitochondrial dysfunction and cell apoptosis [24, 25], we subsequently examined the gene expression of several molecules in MAP, including caspase3, anti-apoptotic protein Bcl-2 and pro-apoptotic protein Bax by western blotting and qRT-PCR. Fig. 2C shows the representative blots images of apoptotic-related proteins. Consistent with previous studies, the ratio of Bax/Bcl-2 was significantly higher in S-8 h group (0.41±0.07, $p<0.05$) and S-24 h group (1.13±0.12, $p<0.001$) (Fig. 2D) compared to the NES controls (0.23±0.04). Protein levels of cleaved caspase3 were also significantly higher in S-8 h group (1.53±0.14, $p<0.001$) and S-24 h group (1.85±0.15, $p<0.001$) compared to those in the NES control group (1.05±0.14, relative to GAPDH) (Fig. 2E). Gene expressions of these molecules were further examined and similar results were obtained: CASPASE3 and BAX were significantly upregulated in the RES groups, while BCL was significantly downregulated (Fig. 2F). Accordingly, RES may elicit damages to mitochondria and promote apoptosis, which may result in cardiomyocyte loss.

RES disrupted cytoplasmic calcium

Several previous studies have claimed that cytoplasmic calcium has an important impact on mitochondrial condition [26-28]. Considering the mitochondrial dysfunction in our study and the importance of calcium to cardiomyocytes, we next examined calcium transients in cardiomyocytes with and without electrical stimulation using Fluo3-AM staining. Fig. 3A shows the typical dynamic evolution of calcium in each group, and the peak value of each curve represents the maximal increase in calcium relative to baseline. Compared to the NES control group, amplitudes of calcium transients in the RES groups were significantly decreased (0.36±0.04, 0.18±0.02, 0.10±0.02 for NES control, S-8 h and S-24 h groups, respectively, $p<0.001$, Fig. 3B).

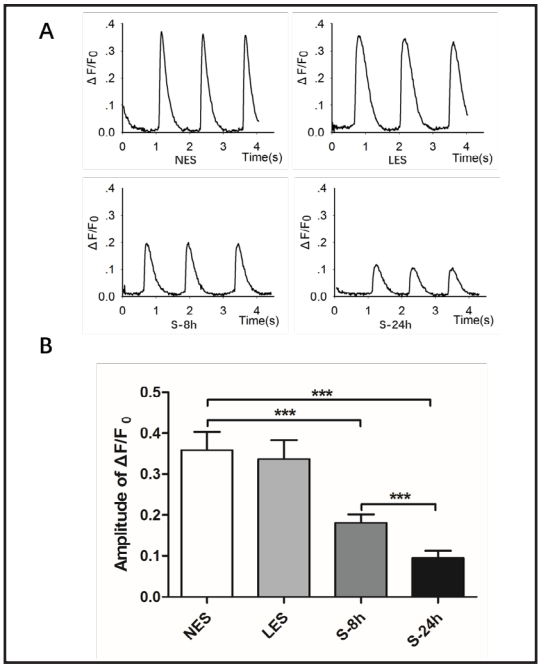

Fig. 3. RES disrupted cytoplasmic calcium. A: Representative calcium transients in each group. Calcium transients were measured using the calcium indicator Fluo-3 AM and expressed as $\Delta F/F_0$, where ΔF is the change in fluorescence intensity of Fluo-3 AM relative to the minimal fluorescence (F_0). B: Quantitative analysis of amplitude of $\Delta F/F_0$. There was a significant time-dependent decrease in amplitudes in RES groups(n=24). **p<0.01, ***p<0.001 tested by one-way ANOVA.

RES decreased L-type calcium currents

We next recorded L-type calcium currents ($I_{Ca,L}$) using patch clamp under voltage clamp mode. Typical traces of $I_{Ca,L}$ and I-V curves of cardiomyocytes in each group are shown in Fig. 4A and 4B; currents were normalized to the capacitance and were expressed in pA/pF as current density. As shown in Fig. 4C, $I_{Ca,L}$ amplitudes in RES groups dramatically decreased compared to the values observed in NES controls (-9.02±0.66 pA/pF, -2.88±0.26 pA/pF, -2.09±0.39 pA/pF for the NES control, S-8 h and S-24 h groups, respectively, $p<0.001$). There was no significant difference between the NES control and LES control groups (-8.56±0.42 pA/pF, $p=0.29$).

Abnormal expression of calcium homeostasis-related genes and proteins

Cytoplasmic calcium is maintained by a balance between the release of Ca^{2+} into the cytosol and the removal of Ca^{2+} by the associated action of some proteins in the cell. Ca^{2+} entry is facilitated by the voltage-sensitive L-type Ca^{2+} channels, which triggers the release of Ca^{2+} from SR through ryanodine receptors (RyR), raising cytoplasmic Ca^{2+} and causing contraction, known as calcium induced calcium release (CICR). Following cardiac contraction, Ca^{2+} is removed from the cytosol primarily in 3 ways: most of it is re-sequenced to the SR via the sarco-endoplasmic reticulum ATPase (Serca), some of it is extruded into the extracellular space through the Na^{+}-Ca^{2+} exchanger (NCX) or Ca^{2+} ATPase pump, and some enters the mitochondria. In the present study, disrupted cytoplasmic calcium and decreased L-type calcium currents indicated disturbed calcium homeostasis. Herein, we then investigated the expression of calcium homeostasis-related proteins and genes using western blotting and qRT-PCR. We first examined the expression of Serca2a and its regulatory protein phospholamban (Pln), which interacts with Serca2a and promotes its pumping activity [29]; the representative blot image of Serca2a and Pln is shown in Fig. 5A. There was a significant reduction in the expression of Serca2a in S-24 h group ($p<0.05$) compared to that in the NES control group; however, no significant reduction in expressions were observed among other groups (Fig. 5B). Cardiomyocytes in RES groups demonstrated significantly lower levels of Pln, which may inhibit the pumping function of Serca2a and the re-sequencing of cytoplasmic calcium. Calsequestrin2 (Casq2), a large-capacity Ca-binding protein which locates in the terminal cisternae of SR, plays a role as a buffer of free Ca^{2+} in the SR and maintains a relatively lower concentration of free Ca^{2+} within the SR, thereby dynamically mediating Ca^{2+} re-sequencing [30]. As seen in Fig. 5A and 5B, protein levels of Casq2 were dramatically decreased in S-8 h ($p<0.05$) and S-24 h groups ($p<0.01$), whereas no decrease was observed in LES control group. These results were further confirmed by qRT-PCR (Fig. 5C).

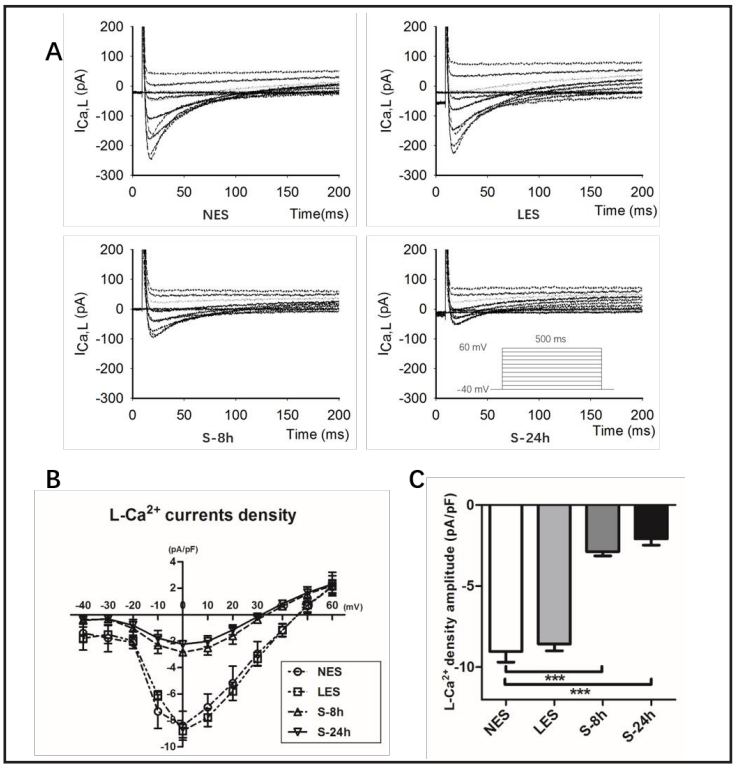

Fig. 4. RES decreased L-type calcium currents. A: Representative L-type calcium currents traces in each group. B: Typical I-V curve of L-type calcium currents. Current densities were normalized to capacitance and expressed in pA/pF as current density. C: Quantitative analysis of amplitude of L-type calcium current density. RES significantly decreased L-type calcium currents amplitude in a time-dependent manner(n=4). ***p<0.001 tested by one-way ANOVA.

CaMKII is a ubiquitous kinase which is canonically activated by the increase of intracellular Ca^{2+}. CaMKII has been reported to be activated in heart failure animal models [31] and patients [32] and is strongly associated with mitochondrial stress [33]. Activation of CaMKII has also been demonstrated to be a common intermediate of variable death stimuli

which induce apoptosis in cardiomyocytes [34]. Hashambhoy YL et al. [35] reported that CaMKII is activated by excessive calcium, and overactivation of CaMKII increases CaMKII-dependent phosphorylation of RyR2 and thus increases the diastolic SR Ca^{2+} leak, which may further increase cytoplasmic calcium and form a vicious cycle. It was demonstrated in our study that the expression of phosphorylated CaMKII was significantly upregulated following RES (Fig. 5).

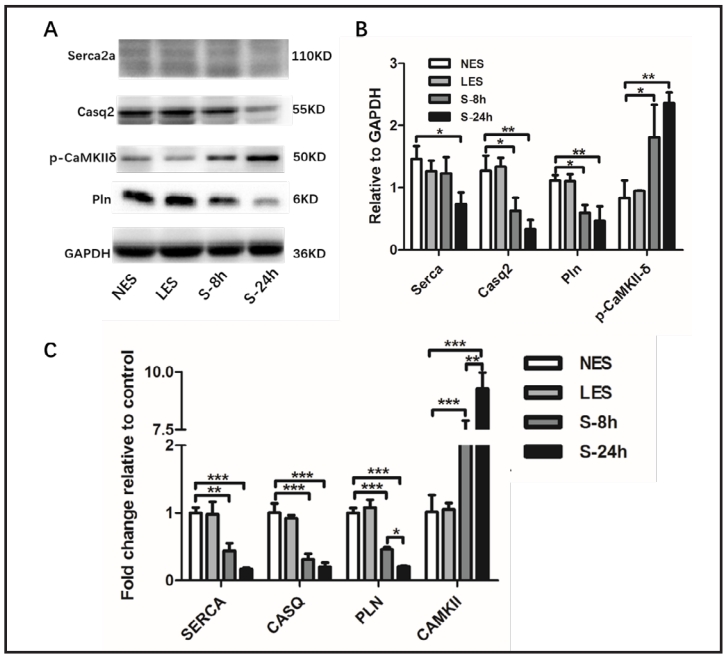

Fig. 5. RES induced abnormal expression of calcium homeostasis-related genes and proteins. A: Representative western blotting image of calcium homeostasis-related proteins. B: Quantitative analysis of protein levels relative to GAPDH. Proteins favor calcium resequencing including Serca2a, Casq and Pln were significantly downregulated in RES groups. GAPDH was used as an internal control(n=3). C: qPCR analysis of homeostasis -related genes(n=3). *p<0.05, **p<0.01, ***p<0.001 tested by one-way ANOVA.

Inhibition of CaMKII partly reversed disturbed calcium homeostasis of RES

Considering that CaMKII inhibitors have been applied for heart failure patients [36, 37], we prescribed 1 μM KN93 based on published studies [38, 39] on S-24 h group cells during RES. As shown in Fig. 6, following KN93 treatment, the maximal $\Delta F/F_0$ values of calcium transients were significantly increased to 0.244±0.028 (p<0.001), indicating that disruption of cytoplasmic calcium was attenuated. Afterwards, L-type calcium currents were also recorded. $I_{Ca,L}$ was significantly increased from -2.04±0.48 pA/pF in S-24 h group to -4.06±1.02 pA/pF in S-24 h+KN93 group (p<0.001, see online suppl. material, Fig. S1); however, the currents in the KN93-treated group were still significantly smaller than those in the NES control group (-8.30±0.85 pA/pF, p<0.001, see online suppl. material, Fig. S1).

Inhibition of CaMKII partly reversed the adverse effects of RES

After confirming the beneficial effects of KN93 on reversing disturbed calcium homeostasis, we investigated whether it also attenuated mitochondrial dysfunction and cardiomyocyte apoptosis induced by RES. As shown in Fig. 7A, compared to the S-24 h group, MMP loss of hiPSC-CMs was significantly attenuated in the KN93-treated cardiomyocytes. The ratio of monomers to aggregates decreased from 2.12±0.42 in S-24 h group to 1.06±0.20 in S-24 h +KN93 group (p<0.01); however, the ratio in the KN93-treated group was still significantly higher compared to that of the NES control group (0.46±0.10, p<0.01), indicating that mitochondrial dysfunction was partly attenuated. Apoptosis in hiPSC-CMs was also examined using Hoechst staining and AV/PI flow cytometry. As shown (see online suppl. material) in Fig. S2 and Fig. 7B, the percentage of apoptotic cells was decreased from 26.82%±3.19% in S-24 h group to 12.93%±1.60% in S-24 h +KN93 group (p<0.001); however, the percentage in the KN93-treated group was still higher than the NES controls (8.58%±2.28%, p<0.01). We further examined the expression of Caspase3, Bax and Bcl-2. As shown in Fig. 7C-F, all the changes caused by RES were significantly attenuated after

treatment with KN93; however, cells did not fully recover to control levels, indicating that some damages caused by RES were irreversible.

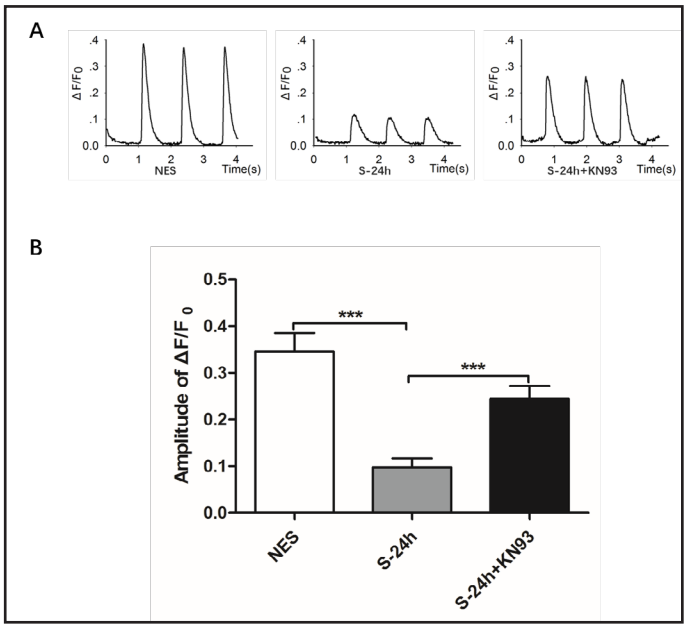

Fig. 6. CaMKII inhibitor KN93 attenuated disturbed calcium homeostasis. A: Representative calcium transients of each group. Calcium transients were measured using the calcium indicator Fluo-3 AM and expressed as $\Delta F/F_0$, where ΔF is the change in fluorescence intensity of Fluo-3 AM relative to the minimal fluorescence (F_0). B: Quantitative analysis of amplitude of $\Delta F/F_0$. Amplitudes were significantly increased after treatment with KN93(n=24). **p<0.01, ***p<0.001 tested by one-way ANOVA.

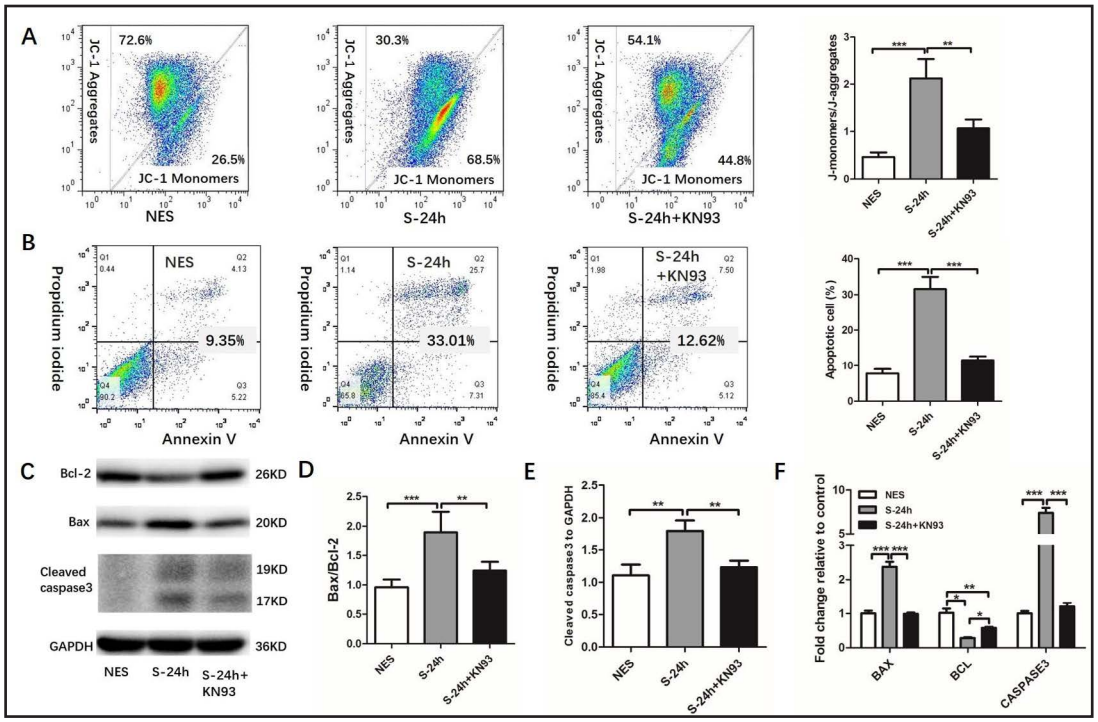

Fig. 7. CaMKII inhibitor KN93 attenuated damages induced by RES. A-B:KN93 partly attenuated MMP loss (A) and reduced apoptotic cardiomyocytes (B) caused by RES(n=4). C: Representative western blotting image of apoptosis-related proteins. D-E: Quantitative analysis of protein levels of apoptosis-related proteins(n=3). Bax and cleaved Caspase3 were upregulated in S-24h+KN93 group compared to the S-24 h group and protein level of Bcl-2 was also increased. F: qPCR analysis of apoptosis-related genes(n=3). *p<0.05, **p<0.01, ***p<0.001 tested by one-way ANOVA.

Discussion

Tachycardia is the most common arrhythmia in clinical practice and has become a huge burden for patients and society in terms of both economics and health. Heart failure induced by tachycardia has been increasingly observed; however, its mechanism remains unclear [1-3]. Many clinicians hold the view that damages induced by tachycardia can be reversed following the termination of tachycardia, but there have been reports of recurrence of tachycardia and sudden cardiac death even after the treatment of tachycardia, which indicates an incomplete recovery [3, 4]. Previously, many efforts have been made to investigate the mechanisms of tachycardia-induced cardiac damages in animal models. Paslawska U et al. [5] observed that swine, after 170 bpm pacing, presented reduced exercise capacity, LV dilatation, impaired LV systolic function and interstitial fibrosis; Kusunose K et al. [7] reported decreased systolic LV strain, loss of early diastolic recoil, and twist deformation. Apart from animal models, there were also various studies investigating tachycardia at the cellular level. Our previous study demonstrated that HL-1 cells, after rapid pacing, presented a greater extent of apoptosis, and the ER stress-mediated MAP and MAPK pathways participated in this process [10]. Using myocytes isolated from Wistar rats, Sepúlveda M et al. [8] discovered that rapid pacing induced CaMKII activation and myocyte apoptosis in a cascade reaction of ROS. However, the precise changes in calcium homeostasis remained unclear. Despite the findings in these studies, an inevitable hurdle is the species differences between animals and human beings. Moreover, cardiomyocytes in these studies were stimulated for 24 hours or even 1 hour, which is an extremely short time for mimicking clinical tachycardia. Owing to the great advances of regenerative medicine, we tried to mimic clinical tachycardia by applying 180 bpm RES on hiPSC-CMs for 1 week. We also divided the cells into two subgroups, S-8 h and S-24 h, to represent short-term and long-term tachycardia. A negative control group receiving 1 Hz stimulation was also established to define whether electrical stimulation itself can bring any changes to cardiomyocytes.

Previously, it was suggested that electrical stimulation promotes cardiac differentiation and maturation of hiPSC-derived cardiomyocytes [40-42]. Ruan et al. [41] reported that electrical stimulation promotes force maturation of induced pluripotent stem cell-derived cardiac tissue; however, the cardiomyocytes used in this study were only 2 or 3 weeks old. Damián Hernández et al. [42] reported that electrical stimulation promoted cardiac differentiation; however, the parameters of electrical stimulation were set at 1 Hz and for a very short period of approximately 15 min. The effects of stimulation when extended to a longer time or on older cardiomyocytes remain unknown. Consistent with previous findings [43, 44] that long-term cultivation promotes maturation of hiPSC-CMs, immunostaining of the cardiac marker cTnT presented clear and organized sarcomeres (see online suppl. material, Fig. S3), which indicated that 8-week-old cardiomyocytes used in our work were relatively mature, and the effects of applying RES on these cells have not been reported.

In our study, amplitudes of calcium transients and L-type calcium currents were significantly decreased following RES in a time-dependent manner (Fig. 3, 4). Genes related to the re-sequencing of calcium including SERCA, CASQ, and PLN were significantly downregulated at both the protein and mRNA levels following RES, these changes disturbed the normal decrease of free calcium in cytoplasm and may explain the disrupted cytoplasmic calcium occurred in the present study. Significant loss in MMP of mitochondria and increased cardiomyocyte apoptosis were observed following RES. Caspase3 and pro-apoptotic Bax were significantly upregulated in RES groups, while anti-apoptotic Bcl-2 was correspondingly downregulated, suggesting the activation of the MAP.

Previously, several studies have reported the relationship between cellular calcium and mitochondria. Vasington and Murphy [45] first demonstrated, at the beginning of the 1960s, that Ca^{2+} is accumulated by the mitochondria. Santulli G et al. [46] further reported that increased cytoplasmic calcium concentration caused mitochondrial Ca^{2+} overloading and dysfunction in a murine model of post-myocardial infarction heart failure. Ca^{2+}

accumulation impairs mitochondrial function, which resulted in reduced ATP production and enhanced release of reactive oxygen species (ROS) [47], and ROS production is closely involved in heart failure [48]. Based on these studies and our present work, we believe that RES-induced cytoplasmic calcium disruption may cause mitochondrial dysfunction and activate MAP, which may lead to cardiomyocyte apoptosis and cell loss.

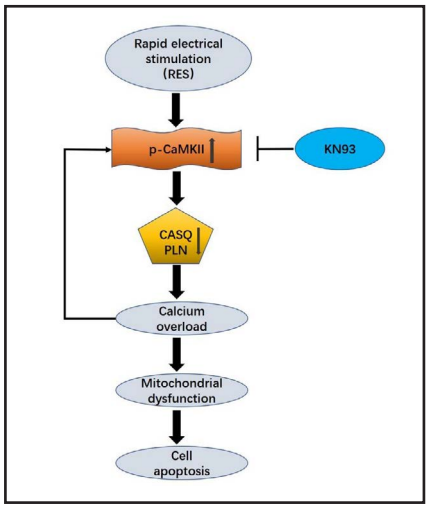

Fig. 8. Illustrated Fig. of RES induced cell apoptosis.

CaMKII, which can be activated by elevated cytoplasmic calcium, is a critical molecule involved in excitation-contraction coupling and calcium homeostasis. It has been previously reported that increased concentration of cytoplasmic Ca^{2+} triggered cell death in several experimental models by activating CaMKII [31, 32]. Upregulated CaMKII phosphorylation can also increase CaMKII-dependent phosphorylation of RyR2 and cause a diastolic SR Ca^{2+} leak and further increase cytoplasmic calcium, thus creating a vicious cycle [35]. Breaking this cycle by inhibition of CaMKII has been reported to benefit heart failure animals and patients [36, 37]. Consistently, KN93, a CaMKII inhibitor, used in our study significantly attenuated adverse effects caused by RES, including calcium transients and L-type calcium currents. Moreover, MMP was increased to levels comparable to that observed in NES controls, meanwhile apoptotic cell rates were significantly decreased. MAP molecules, Caspase3 and Bax were observed to be downregulated compared to their levels in S-24 h group, while Bcl-2 was upregulated. However, these recoveries were incomplete compared to the levels observed in the NES control group, indicating that some damages were irreversible.

Taking together, we demonstrated that RES disturbed calcium homeostasis and resulted in mitochondrial dysfunction and promoted cell apoptosis. Phosphorylated CaMKII was upregulated under RES and inhibition of CaMKII with KN93 partly attenuate the adverse effects of RES.

Conclusion

In summary, as shown in the illustrated Fig. (Fig. 8), rapid electrical stimulation on hiPSC-CMs disturbed calcium homeostasis, which led to mitochondrial stress and promoted cell apoptosis and caused electrophysiological remodeling in a time-dependent manner. CaMKII played a central role in the damages induced by RES, and pharmacological inhibition of CaMKII activity partly reversed the adverse effects on both structural and electrophysiological properties, which could be chosen as a possible supplemental therapeutic target for tachycardia patients.

Acknowledgements

This work was supported by grants from National Natural and Science Foundation of China (grant number 81400249 and 81470455 to ZW and MC, http://www.nsfc.gov.cn/), China Postdoctoral Science Foundation (grant number 2016 M601852 to JW, http://www.chinapostdoctor.org.cn/) and Natural Science Foundation of Jiangsu Province of China (grant number BK2016060 to JS, http://www.jstd.gov.cn/).

Disclosure Statement

There is no conflict of interests.

References

1 Khasnis A, Jongnarangsin K, Abela G, Veerareddy S, Reddy V, Thakur R: Tachycardia-induced cardiomyopathy: A review of literature. Pacing Clin Electrophysiol 2005;28:710-721.
2 Lashus AG, Case CL, Gillette PC: Catheter Ablation Treatment of Supraventricular Tachycardia-Induced Cardiomyopathy. Arch Pediatr Adolesc Med 1997;151:264-266.
3 Ling LH, Kalman JM, Ellims AH, Iles LM, Medi C, Sherratt C, Kaye DM, Hare JL, Kistler PM, Taylor AJ: Diffuse Ventricular Fibrosis Is a Late Outcome of Tachycardia-Mediated Cardiomyopathy After Successful Ablation. Circ Arrhythm Electrophysiol 2013;6:697-704.
4 Nerheim P, Birger-Botkin S, Piracha L, Olshansky B: Heart failure and sudden death in patients with tachycardia-induced cardiomyopathy and recurrent tachycardia. Circulation 2004;110:247-252.
5 Paslawska U, Gajek J, Kiczak L, Noszczyk-Nowak A, Skrzypczak P, Bania J, Tomaszek A, Zacharski M, Sambor I, Dziegiel P, Zysko D, Banasiak W, Jankowska EA, Ponikowski P: Development of porcine model of chronic tachycardia-induced cardiomyopathy. Int J Cardiol 2011;153:36-41.
6 Timek TA, Dagum P, Lai DT, Liang D, Daughters GT, Tibayan F, Ingels NB Jr, Miller DC: Tachycardia-induced cardiomyopathy in the ovine heart: mitral annular dynamic three-dimensional geometry. J Thorac Cardiovasc Surg 2003;125:315-324.
7 Kusunose K, Zhang Y, Mazgalev TN, Thomas JD, Popović ZB: Left ventricular strain distribution in healthy dogs and in dogs with tachycardia-induced dilated cardiomyopathy. Cardiovasc Ultrasound 2013;11:43.
8 Sepúlveda M, Gonano LA, Back TG, Chen SR, Vila Petroff M: Role of CaMKII and ROS in rapid pacing-induced apoptosis. J Mol Cell Cardiol 2013;63:135-145.
9 Yang Z, Shen W, Rottman JN, Wikswo JP, Murray KT: Rapid stimulation causes electrical remodeling in cultured atrial myocytes. J Mol Cell Cardiol 2005;38:299-308.
10 Shi J, Jiang Q, Ding X, Xu W, Wang DW, Chen M: The ER Stress-Mediated Mitochondrial Apoptotic Pathway and MAPKs Modulate Tachypacing-Induced Apoptosis in HL-1 Atrial Myocytes. PLoS One 2015;10:e0117567.
11 Ma J, Guo L, Fiene SJ, Anson BD, Thomson JA, Kamp TJ, Kolaja KL, Swanson BJ, January CT: High purity human-induced pluripotent stem cell-derived cardiomyocytes: electrophysiological properties of action potentials and ionic currents. Am J Physiol Heart Circ Physiol 2011;301:H2006–H2017.
12 Liang P, Lan F, Lee AS, Gong T, Sanchez-Freire V, Wang Y, Diecke S, Sallam K, Knowles JW, Wang PJ, Nguyen PK, Bers DM, Robbins RC, Wu JC: Drug Screening Using a Library of Human Induced Pluripotent Stem Cell-Derived Cardiomyocytes Reveals Disease Specific Patterns of Cardiotoxicity. Circulation 2013;127:1677-1691.
13 Karakikes I, Ameen M, Termglinchan V, Wu JC: Human Induced Pluripotent Stem Cell-Derived Cardiomyocytes: Insights into Molecular, Cellular, and Functional Phenotypes. Circ Res 2015;117:80-88.
14 Hwang HS, Kryshtal DO, Feaster TK, Sánchez-Freire V, Zhang J, Kamp TJ, Hong CC, Wu JC, Knollmann BC: Comparable calcium handling of human iPSC-derived cardiomyocytes generated by multiple laboratories. J Mol Cell Cardiol 2015;85:79–88.
15 Sharma A, Li G, Rajarajan K, Hamaguchi R, Burridge PW, Wu SM: Derivation of highly purified cardiomyocytes from human induced pluripotent stem cells using small molecule-modulated differentiation and subsequent glucose starvation. J Vis Exp DOI: 10.3791/52628.
16 Burridge PW, Holmström A, Wu JC: Chemically Defined Culture and Cardiomyocyte Differentiation of Human Pluripotent Stem Cells. Curr Protoc Hum Genet 2015;87:21.3.1-15.
17 Wang J, Cui C, Nan H, Yu Y, Xiao Y, Poon E, Yang G, Wang X, Wang C, Li L, Boheler KR, Ma X, Cheng X, Ni Z, Chen M: Graphene Sheet-Induced Global Maturation of Cardiomyocytes Derived from Human Induced Pluripotent Stem Cells. ACS Appl Mater Interfaces 2017;9:25929-25940.
18 Birner C, Dietl A, Deutzmann R, Schröder J, Schmid P, Jungbauer C, Resch M, Endemann D, Stark K, Riegger G, Luchner A: Proteomic profiling implies mitochondrial dysfunction in tachycardia-induced heart failure. J Card Fail 2012;18:660-673.

19 Zhong JQ, Zhang W, Gao H, Li Y, Zhong M, Li D, Zhang C, Zhang Y: Changes in connexin 43, metalloproteinase and tissue inhibitor of metalloproteinase during tachycardia-induced cardiomyopathy in dogs. Eur J Heart Fail 2007;9:23-29.
20 Mueller K AL, Heinzmann D, Klingel K, Fallier-Becker P, Kandolf R, Kilias A, Walker-Allgaier B, Borst O, Kumbrink J, Kirchner T, Langer H, Geisler T, Schreieck J, Gramlich M, Gawaz M, Seizer P: Histopathological and Immunological Characteristics of Tachycardia-Induced Cardiomyopathy. J Am Coll Cardiol 2017;69:2160-2172.
21 Gerloni R, Abate E, Pinamonti B, Milo M, Benussi B, Poletti A, Pappalardo A, Bussani R, Sinagra G: A life-threatening manifestation of tachycardia-induced cardiomyopathy. J Cardiovasc Med (Hagerstown) 2014;15:164-166.
22 Nishikawa T, Ishiyama S, Sakomura Y, Nakazawa M, Momma K, Hiroe M, Kasajima T: Histopathologic aspects of endomyocardial biopsy in pediatric patients with idiopathic ventricular tachycardia. Pediatr Int 1999;41:534-537.
23 Nazeri A, Elayda MA, Segura AM, Stainback RF, Nathan J, Lee VV, Bove C, Sampaio L, Grace B, Massumi A, Razavi M: Comparative Efficacy of Nebivolol and Metoprolol to Prevent Tachycardia-Induced Cardiomyopathy in a Porcine Model. Tex Heart Inst J 2016;43:477-481.
24 Zhang BF, Xing L, Cui PF, Wang FZ, Xie RL, Zhang JL, Zhang M, He YJ, Lyu JY, Qiao JB, Chen BA, Jiang HL: Mitochondria apoptosis pathway synergistically activated by hierarchical targeted nanoparticles co-delivering siRNA and lonidamine. Biomaterials 2015;61:178-189.
25 Sreedhar R, Arumugam S, Thandavarayan RA, Giridharan VV, Karuppagounder V, Pitchaimani V, Afrin R, Miyashita S, Nomoto M, Harima M, Gurusamy N, Suzuki K, Watanabe K: Myocardial 14-3-3η protein protects against mitochondria mediated apoptosis. Cell Signal 2015;27:770-776.
26 Lavorato M, Iyer VR, Dewight W, Cupo RR, Debattisti V, Gomez L, De la Fuente S, Zhao YT, Valdivia HH, Hajnóczky G, Franzini-Armstrong C: Increased mitochondrial nanotunneling activity, induced by calcium imbalance, affects intermitochondrial matrix exchanges. Proc Natl Acad Sci U S A 2017;114:E849-E858.
27 Parra V, Moraga F, Kuzmicic J, López-Crisosto C, Troncoso R, Torrealba N, Criollo A, Díaz-Elizondo J, Rothermel BA, Quest AF, Lavandero S: Calcium and mitochondrial metabolism in ceramide-induced cardiomyocyte death. Biochim Biophys Acta 2013;1832:1334-1344.
28 Zhang XH, Haviland S, Wei H, Sarić T, Fatima A, Hescheler J, Cleemann L, Morad M: Ca^{2+} signaling in human induced pluripotent stem cell-derived cardiomyocytes (iPS-CM) from normal and catecholaminergic polymorphic ventricular tachycardia (CPVT)-afflicted subjects. Cell Calcium 2013;54:57-70.
29 Kranias EG, Hajjar RJ: Modulation of cardiac contractility by the phospholamban/SERCA2a regulatome. Circ Res 2012;110:1646-1660.
30 Faggioni M, Knollmann BC: Calsequestrin 2 and arrhythmias. Am J Physiol Heart Circ Physiol 2012;302:H1250-1260.
31 Kreusser MM, Lehmann LH, Keranov S, Hoting MO, Oehl U, Kohlhaas M, Reil JC, Neumann K, Schneider MD, Hill JA, Dobrev D, Maack C, Maier LS, Gröne HJ, Katus HA, Olson EN, Backs J: Cardiac CaM Kinase II genes δ and γ contribute to adverse remodeling but redundantly inhibit calcineurin-induced myocardial hypertrophy. Circulation 2014;130:1262-1273.
32 Hoch B, Meyer R, Hetzer R, Krause EG, Karczewski P: Identification and expression of delta-isoforms of the multifunctional Ca^{2+}/calmodulin dependent protein kinase in failing and nonfailing human myocardium. Circ Res 1999;84:713-721.
33 Joiner ML, Koval OM, Li J, He BJ, Allamargot C, Gao Z, Luczak ED, Hall DD, Fink BD, Chen B, Yang J, Moore SA, Scholz TD, Strack S, Mohler PJ, Sivitz WI, Song LS, Anderson ME: CaMKII determines mitochondrial stress responses in heart. Nature 2012;491:269-273.
34 Zhu W, Woo AY, Yang D, Cheng H, Crow MT, Xiao RP: Activation of CaMKII deltaC is a common intermediate of diverse death stimuli-induced heart muscle cell apoptosis. J Biol Chem 2007;282:10833-10839.
35 Hashambhoy YL, Greenstein JL, Winslow RL: Role of CaMKII in RyR leak, EC coupling and action potential duration: a computational model. J Mol Cell Cardiol 2010;49:617-624.
36 Fischer TH, Kleinwächter A, Herting J, Eiringhaus J, Hartmann N, Renner A, Gummert J, Haverich A, Schmitto JD, Sossalla S: Inhibition of CaMKII Attenuates Progressing Disruption of Ca^{2+} Homeostasis Upon Left Ventricular Assist Device Implantation in Human Heart Failure. Artif Organs 2016;40:719-726.

37 Sossalla S, Fluschnik N, Schotola H, Ort KR, Neef S, Schulte T, Wittköpper K, Renner A, Schmitto JD, Gummert J, El-Armouche A, Hasenfuss G, Maier LS: Inhibition of elevated Ca^{2+}/calmodulin-dependent protein kinase II improves contractility in human failing myocardium. Circ Res 2010;107:1150-1161.
38 Rezazadeh S, Claydon TW, Fedida D: KN-93 (2-[N-(2-hydroxyethyl)]-N-(4-methoxybenzenesulfonyl)] amino-N-(4-chlorocinnamyl)-N-methylbenzylamine), a calcium/calmodulin-dependent protein kinase II inhibitor, is a direct extracellular blocker of voltage-gated potassium channels. J Pharmacol Exp Ther 2006;317:292-299.
39 Brooks IM, Tavalin SJ: Ca^{2+}/Calmodulin-dependent Protein Kinase II Inhibitors Disrupt AKAP79-dependent PKC Signaling to GluA1 AMPA Receptors. J Biol Chem 2011;286:6697-6706.
40 Ma R, Liang J, Huang W, Guo L, Cai W, Wang L, Paul C, Yang HT, Kim HW, Wang Y: Electric stimulation enhances cardiac differentiation of human induced pluripotent stem cells for myocardial infarction therapy stem cells for myocardial infarction. Antioxid Redox Signal 2017;28:371-384.
41 Ruan JL, Tulloch NL, Razumova MV, Saiget M, Muskheli V, Pabon L, Reinecke H, Regnier M, Murry CE: Mechanical Stress Conditioning and Electrical Stimulation Promote Contractility and Force Maturation of Induced Pluripotent Stem Cell-Derived Human Cardiac Tissue. Circulation 2016;134:1557-1567.
42 Hernández D, Millard R, Sivakumaran P, Wong RC, Crombie DE, Hewitt AW, Liang H, Hung SS, Pébay A, Shepherd RK, Dusting GJ, Lim SY: Electrical Stimulation Promotes Cardiac Differentiation of Human Induced Pluripotent Stem Cells. Stem Cells Int 2016;2016:1718041.
43 Lundy SD, Zhu WZ, Regnier M, Laflamme MA: Structural and functional maturation of cardiomyocytes derived from human pluripotent stem cells. Stem Cells Dev 15;22:1991-2002.
44 Kamakura T, Makiyama T, Sasaki K, Yoshida Y, Wuriyanghai Y, Chen J, Hattori T, Ohno S, Kita T, Horie M, Yamanaka S, Kimura T: Ultrastructural maturation of human-induced pluripotent stem cell-derived cardiomyocytes in a long-term culture. Circ J 2013;77:1307-1314.
45 Vasington FD, Murphy JV: Ca ion uptake by rat kidney mitochondria and its dependence on respiration and phosphorylation. J Biol Chem 1962;237:2670-2677.
46 Santulli G, Xie W, Reiken SR, Marks AR: Mitochondrial calcium overload is a key determinant in heart failure. Proc Natl Acad Sci U S A 2015;112:11389-11394.
47 Orrenius S, Gogvadze V, Zhivotovsky B: Calcium and mitochondria in the regulation of cell death. Biochem Biophys Res Commun 2015;460:72-81.
48 Hafstad AD, Nabeebaccus AA, Shah AM: Novel aspects of ROS signalling in heart failure. Basic Res Cardiol 2013;108:359.